Direct Dark Matter Search with XENON

T. Marrodán Undagoitia[1]
on behalf of the XENON collaboration

[1]Max-Planck-Institut für Kernphysik, Saupfercheckweg 1, 69117 Heidelberg, Germany

DOI: http://dx.doi.org/10.3204/DESY-PROC-2013-04/marrodan_undagoitia_teresa

Direct dark matter searches using liquid xenon have shown a great potential to detect WIMPs (Weakly Interacting Massive Particles) via elastic scattering off the target nuclei. XENON100 operates with an active volume of 62 kg liquid xenon and it is located at the Gran Sasso underground laboratory in Italy. So far the data released provides no evidence for dark matter. The resulting exclusion limits on the WIMP-nucleon cross section for spin-dependent and -independent interactions probe already significant regions of the cross section and WIMP mass parameter space. The XENON1T experiment currently under construction will improve the current sensitivity by two orders of magnitude.

1 Introduction

Cosmological and astronomical observations indicate that a large fraction of the matter in the universe is non baryonic. A common assumption states that dark matter consists of elemental particles which arise naturally in various theories beyond the standard model of particle physics [1]. Weakly Interacting Massive Particles (WIMPs) could interact elastically with target nuclei allowing to detect them directly. Such a measurement would provide information on the interaction probability of WIMPs with ordinary matter and on the WIMP mass. The detection is however challenging as the recoiling nucleus would deposit only a few keV energy and the predicted interaction rate is very low. Therefore, the required detectors need to have a low energy threshold, a large mass and a very low background. Among the various detector technologies currently in use, liquid xenon (LXe) combines a high WIMP sensitivity with an excellent self-shielding capability for background reduction. Its scintillation light at 178 nm can be detected directly with photomultipliers (PMTs) without wavelength-shifter. Furthermore, natural xenon contains almost 50% of non zero spin isotopes, ^{129}Xe and ^{131}Xe, providing sensitivity to spin-dependent WIMP interactions [2].

2 The XENON100 instrument

The XENON100 detector consist of a two-phase liquid xenon time projection chamber (TPC). If a charged particle deposits energy in the medium, not only excitation but also ionisation of the xenon atoms occur. This provides discrimination between signal and background events based on the simultaneous detection of the prompt scintillation light (S1) and the charge signal from electrons released. These electrons are drifted in an electric field and extracted into the gas phase, where the charge is converted via proportional scintillation in the gas to an amplified secondary light signal (S2). Both signals are measured by two arrays of R8520 Hamamatsu PMTs placed on top and bottom of the TPC. The interaction vertices can be reconstructed with few mm precision based on the drift time (time difference between S1 and S2) and the PMT hit pattern of the S2 signal [3].

The detector is located at the Laboratori Nazionale del Gran Sasso in Italy. The total mass of liquid xenon is 161 kg of which 62 kg are contained inside the TPC. The remaining 99 kg of the xenon are used as an active veto surrounding the TPC. The whole system is placed inside a shield consisting of an inner copper layer, lead, polyethylene and an outer neutron shield. Due to a careful screening and selection of radio-pure detector materials, the experiment achieved an electronic recoil background of 5.3×10^{-3} events$\cdot$ kg$^{-1}\cdot$ keV^{-1} in the WIMP-search energy range for a 34 kg fiducial mass [4].

3 Dark matter searches with XENON100

During 2011 and 2012, a science run with a total of 225 life days was acquired [4]. Compared to the previous run, the krypton content was reduced to (19 ± 4) ppt $^{\mathrm{nat}}$Kr in xenon resulting in a subdominant ^{85}Kr contamination. Additionally, the ionisation threshold was lowered by using a new hardware trigger such that the efficiency was $> 99\%$ at 150 photoelectrons (PE) in S2.

The detector is calibrated with ^{137}Cs, ^{60}Co, ^{232}Th (gamma) and ^{241}AmBe (neutron) sources in order to characterize the detector performance, to determine the data selection criteria for dark matter searches and to define the signal and background regions. The region of interest for WIMP candidates was blinded to avoid bias during the analysis. The used science data were selected from periods of stable operating conditions. The criteria to select candidate events include data quality, energy range in S1 and S2, selection of single scatter events, consistency cuts and analysis volume [6]. The acceptance for these cuts was calculated using mainly nuclear recoils from calibration data. The nuclear recoil scale E_{nr} was calculated from the light signal (S1) using the equation $E_{nr} = (\mathrm{S1}/L_y)(1/L_{eff})(S_{ee}/S_{nr})$ where L_y is the light yield of a 122 keV gamma ray at zero applied drift field. The term L_{eff} accounts for all quenching effects of the nuclear recoil scale and it is parametrized using all existing measurements from neutron scattering experiments (see [5] and references therein). S_{ee} and S_{nr} are the electric field scintillation quenching factors for electronic recoils and nuclear recoils.

A profile likelihood method was use to test both the signal and the background-only hypothesis in the predefined energy range $(3-30)$ PE corresponding to $(6.6-43.3)\,\mathrm{keV}_{nr}$ recoil energy. The background prediction included electronic recoil leakage from the main background region and nuclear recoils from neutrons reaching the innermost 34 kg mass used for the analysis. After unblinding, the profile likelihood analysis yielded a $p-$value of $\leq 5\%$ for all WIMP masses indicating no signal over the predicted background.

This result was interpreted in terms of spin-independent [4] and -dependent [2] interactions of WIMPs. Figure 1 shows the expected sensitivity bands ($1\,\sigma$ in green and $2\,\sigma$ in yellow) together with the actual exclusion limits for spin-independent (left) and neutron coupling spin-dependent (right) WIMP-nucleon cross sections. The shaded gray regions represent theoretically favoured regions in this parameter space. The closed regions represent the $2\,\sigma$ signal indications from the DAMA, CoGeNT and CRESST-II experiments (see references in [4]) which are in tension with the result of XENON100.

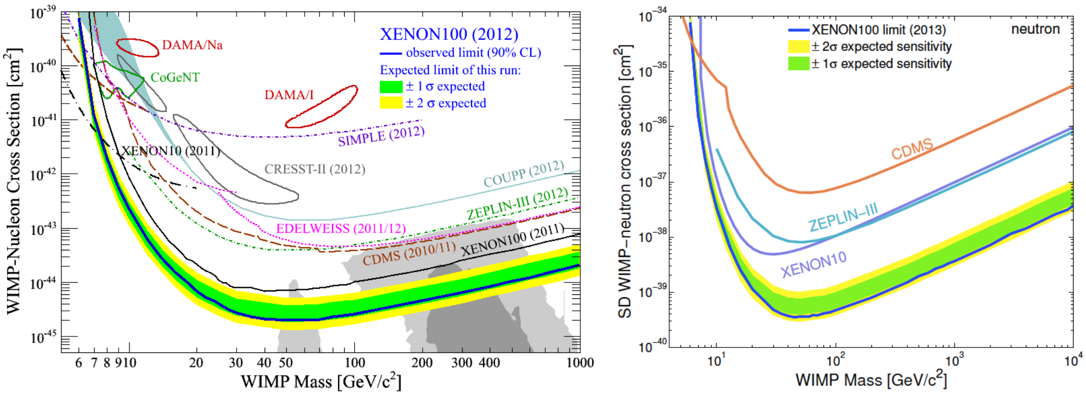

Figure 1: WIMP-nucleon cross section exclusion limits from 225 live days run of XENON100. (Left) Spin-independent. (Right) Spin-dependent (neutron coupling). Figures from [4] and [2], respectively.

3.1 Verification of nuclear recoil energy scale

A data/Monte Carlo comparison of the XENON100 nuclear recoil data acquired during the neutron source calibration with ^{241}AmBe has been performed [7] in order to verify the energy scale used for the results mentioned above. The response of the XENON100 experiment was modelled using a detailed geometry of the whole experiment including the shield and the generation of the two signals S1 and S2. The calculated acceptance for the data was also applied to the Monte Carlo generated events.

In a first step, the S2 Monte Carlo spectrum is fitted to the corresponding data. From this procedure, the number of free electrons per unit energy, charge yield Q_y, is extracted (see Figure 2, left). Best spectral matching was obtained for a neutron source rate of 159 n/s.

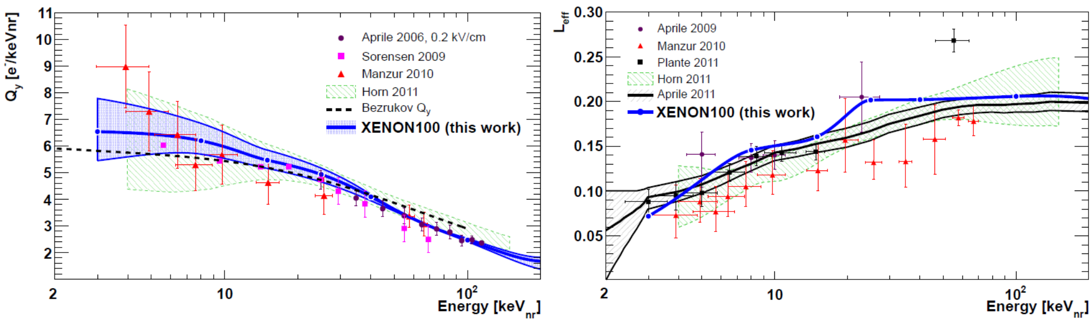

Figure 2: (Left) Q_y obtained from fitting data to the Monte Carlo generated S2 spectrum. (Right) L_{eff} obtained from the Monte Carlo/data matching of the S1 spectrum. Figures from [7].

This number is in agreement with an independent measurement of the rate which yielded (160 ± 4) n/s. Using the derived Q_y, the S1 spectrum of the ^{241}AmBe nuclear recoils is similarly fitted to the Monte Carlo data and the scintillation efficiency L_{eff} is calculated. As it can be seen in Figure 2 (right), the best-fit curve is in agreement with the energy scale used in previous XENON100 analysis [4]. In both mentioned steps, a very good level of spectral shape matching is accomplished along with agreement in the 2-dimensional particle discrimination space (S2 versus S1). These results confirmed the validity of the calculated signal acceptance used by XENON100 for WIMP searches.

4 Determination of the LXe electronic recoil energy scale

In the sections above, the elastic scattering of WIMP particles off nuclei have been considered where the signal signature consists of a nuclear recoil. However, dark matter particle candidates such as axions or axion-like particles [8] would interact predominantly with shell electrons in the target. In order to study the sensitivity of XENON100 to electronic interactions, the response of liquid xenon down to ∼ keV electronic recoil energies needs to be measured.

Recently, laboratory experiments have shown [9][10] that at zero drift field, the light yield at 10 keV decreases below to 40% of its value at higher energies. These experiments use a strong gamma which interacts via Compton scattering in LXe and is then detected in an additional coincidence detector. Using an applied electric field of 450 V/cm [9] which is close to the field of 530 V/cm used in XENON100, the scintillation output is reduced to about 75% relative to the value at zero field. Figure 3 shows the energy dependence of the light yield at zero field (left) and the energy dependence of the field quenching at 450 V/cm. Despite of the light yield

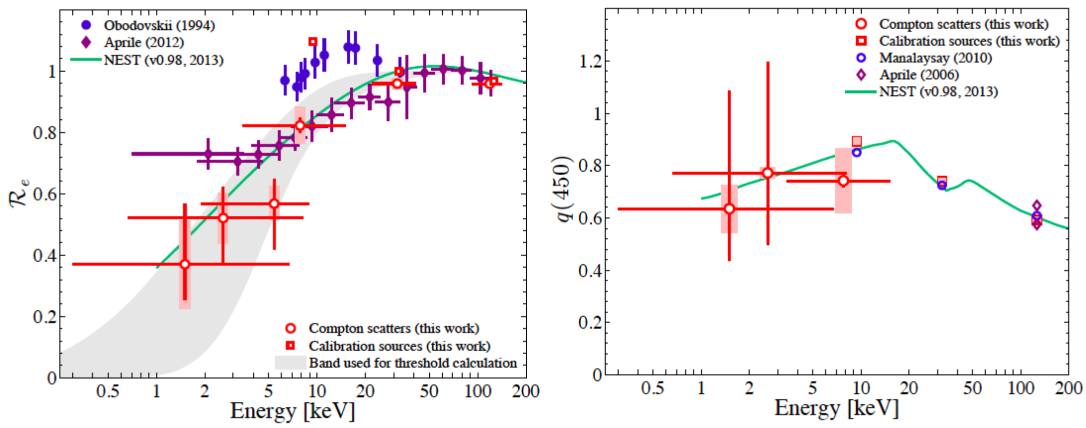

Figure 3: (Left) Energy dependence of the scintillation yield for electronic recoils. (Right) Field quenching at 450 V/cm for different energies. Figures from [9].

reduction mentioned above, liquid xenon shows scintillation at few keV energies in a presence of the tested drift field. Using the data of figure 3, the estimated electronic-recoil energy threshold for XENON100 has been calculated to be at about 2.3 keV.

5 Status of XENON1T

Currently, XENON100 continues being operational and is taking dark matter data. However, in order to increase the sensitivity significantly, the XENON collaboration proposed a next generation detector, XENON1T [11], consisting of about 3 tons of LXe. The design consists of a dual-phase TPC of about 1 m height and about 1 m in diameter. The goal is to reduce the background by a factor of ~ 100 compared to the one of XENON100 which is at the level of 5×10^{-3} events/(keV·kg·d) [4]. This is achieved by using an additional water muon-veto detector, an improved material screening and selection and by reducing the intrinsic contamination with ^{85}Kr and radon using dedicated devices. In addition, a 3 inch high quantum efficiency and low radioactive PMT (Hamamatsu R11410 [12]) will be use to further reduce the background.

XENON1T's goal is to probe spin-independent WIMP-nucleon cross sections down to 2×10^{-47} cm^2 for a 50 GeV/c^2 WIMP mass. Figure 4 shows the projected sensitivity using 2.2 ton-year exposure, 99.75% background rejection rejection in log(S2/S1) parameter space and 40% efficiency to detect nuclear recoils. The construction of the infrastructure for XENON1T has

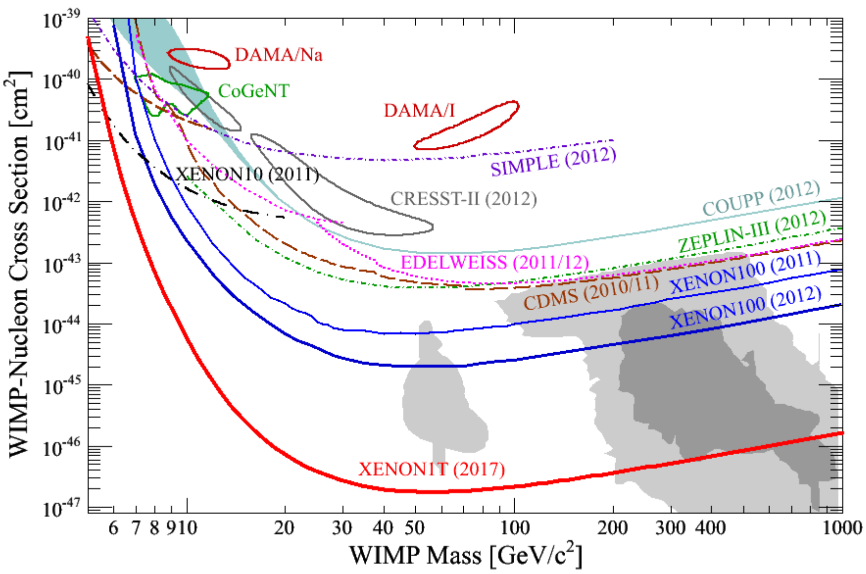

Figure 4: Projected sensitivity for spin independent WIMP-nucleon cross section with the XENON1T experiment.

started this summer at the Laboratori Nationale dell Gran Sasso in Italy and by the time of writing (September 2013) the upper part of the water tank is completed. The start of data taking is planned for 2015.

References

[1] G. Bertone, D. Hooper, and J. Silk, Phys. Rep. **405**, 279 (2005).

[2] E. Aprile *et al.* [XENON100 Collaboration], Phys. Rev. Lett. **111**, 021301 (2013) [arXiv:1301.6620].

[3] E. Aprile *et al.* [XENON100 Collaboration], Astropart. Phys. **35**, 573 (2012) [arXiv:1107.2155].

[4] E. Aprile *et al.* [XENON100 Collaboration], Phys. Rev. Lett. **109**, 181301 (2012) [arXiv:1207.5988].

[5] G. Plante, E. Aprile, R. Budnik, B. Choi, K. L. Giboni, L. W. Goetzke, R. F. Lang and K. E. Lim *et al.*, Phys. Rev. C **84**, 045805 (2011) [arXiv:1104.2587].

[6] E. Aprile *et al.* [XENON100 Collaboration], (2012) [arXiv:1207.3458].

[7] E. Aprile *et al.* [XENON100 Collaboration], Phys. Rev. D **88**, 012006 (2013) [arXiv:1304.1427].

[8] F. T. Avignone *et al.* Phys. Rev. D **35**, 27522757 (1987)

[9] L. Baudis, H. Dujmovic, C. Geis, A. James, A. Kish, A. Manalaysay, T. Marrodán Undagoitia and M. Schumann, Phys. Rev. D **87**, 115015 (2013) [arXiv:1303.6891].

[10] E. Aprile, R. Budnik, B. Choi, H. A. Contreras, K. L. Giboni, L. W. Goetzke, J. E. Koglin and R. F. Lang *et al.*, Phys. Rev. D **86**, 112004 (2012) [arXiv:1209.3658].

[11] E. Aprile *et al.* [XENON1T Collaboration], (2012) [arXiv:1206.6288].

[12] L. Baudis, A. Behrens, A. Ferella, A. Kish, T. Marrodán Undagoitia, D. Mayani and M. Schumann, JINST **8**, P04026 (2013) [arXiv:1303.0226].